

# Evaluating the accuracy of gridded water resources reanalysis and evapotranspiration products for assessing water security in poorly gauged basins

Elias Nkiaka<sup>1</sup>, Robert G. Bryant<sup>1</sup>, Joshua Ntajal<sup>2,3</sup>, Eliezer I. Biao<sup>4</sup>

<sup>1</sup>Department of Geography, University of Sheffield, Sheffield, S10 2TN, UK

<sup>2</sup>Department of Geography, University of Bonn, 53115 Bonn, Germany

<sup>3</sup>Center for Development Research, University of Bonn, 53113 Bonn, Germany

<sup>4</sup>Laboratory of Applied Hydrology, University of Abomey-Calavi (UAC), Cotonou, Benin

Elias Nkiaka (Corresponding author): [e.nkiaka@sheffield.ac.uk](mailto:e.nkiaka@sheffield.ac.uk)

Postal Address: Department of Geography, University of Sheffield, Sheffield, S10 2TN, UK

## Abstract

Achieving water security in poorly gauged basins is critically hindered by a lack of in situ river discharge data to assess past, current and future evolution of water resources. To overcome this challenge, there has been a shift toward the use of freely available satellite and reanalysis data products. However, due to inherent bias and uncertainty, these secondary sources require careful evaluation to ascertain their performance before being applied in poorly gauged basins. The objectives of this study were to evaluate river discharge and evapotranspiration estimates from eight gridded water resources reanalysis (WRR), six satellite-based evapotranspiration (ET) products and ET estimates derived from complimentary relationship (CR-ET) across eight river basins located in Central-West Africa. Results highlight strengths and weaknesses of the different WRR in simulating discharge dynamics and ET across the basins. Likewise satellite-based products also show some strength and weaknesses in simulating monthly ET. Our results further revealed that the performance of the different models in simulating river discharge and evapotranspiration is strongly influenced by model structure, input data and spatial resolution. Considering all hydrological model evaluation criteria, FLDAS-Noah, Lisflood, AWRAL, and Terra were among the best performing WRR products while for ET estimates, FLDAS-Noah, Terra, GLEAM3.5a & 3.5b, and PMLV2 outperformed the rest of the products. Given the plethora of WRR and ET products available, it is imperative to evaluate their performance in representative gauged basins to identify products that can be applied in each region. However, the choice of a particular product will depend on the application and users requirements. Taking together, results from this study suggest that gridded WRR and ET products are a useful source of data for assessing water security in poorly gauged basins.

## 33 **1. Introduction**

34 River discharge is one of the most important hydrological variables underpinning water resources  
35 management, aquatic ecosystems sustainability, flood prediction, and drought warnings at different  
36 scales (McNally et al., 2017; Couasnon et al., 2020). However, observed river discharge data is often  
37 not available at the exact location where critical water management decisions need to be made (Neal  
38 et al., 2009). This is especially the case in developing and semi arid/arid regions where discharge  
39 gauging stations are sparse (Krabbenhof et al., 2022), while the number of existing stations are  
40 declining (Rodríguez et al., 2020). Despite the acute shortage in observed data, developing regions  
41 are areas that are more vulnerable to adverse hydroclimatological conditions (Byers et al., 2018;  
42 Kabuya et al., 2020). Furthermore, achieving water security in poorly gauged basins remains a critical  
43 development challenge as climate change, population growth, rapid urbanization, and economic  
44 growth continue to exert pressure on available water resources under hydrological uncertainty (Flörke  
45 et al., 2018; Hirpa et al., 2019). This highlights the urgent need for more reliable data to better assess  
46 past, current, and future evolution of water resources, and to predict extreme hydroclimatological  
47 events so that better strategies can be put in place to enhance water management and mitigate the  
48 impact of extreme events (Nkiaka et al., 2020; Slater et al., 2021). Water security in this study refers  
49 to the availability of sufficient quantities of water for human use and ecosystem sustainability.

50 Evapotranspiration (ET) is another important hydrological variable that represents the linkage  
51 between water, energy and carbon cycles and ecosystem services and is the second largest process in  
52 the hydrological cycle after precipitation (Zhang et al., 2019). Therefore, ET plays a critical role in  
53 water availability at different scales. As such, accurate estimates of ET are also crucial for water  
54 management operations such as basin-scale water balance estimation, irrigation planning, estimating  
55 water footprint, and assessing the impact of climate change on water availability. However, globally,  
56 in situ ET monitoring stations are also scarce while the existing monitoring network cannot provide  
57 sufficient information on the temporal and spatial trends of ET at large scales (Laipelt et al., 2021).  
58 ET data scarcity may therefore limit our ability to understand changes in the hydrological cycle and  
59 water security in the context of environmental change and hydrological uncertainty.

60 To enhance water security in poorly gauged basins, there has been a progressive shift toward  
61 the use of gridded data derived from satellite and reanalysis (Odusanya et al., 2019; Nkiaka, 2022).  
62 This is because gridded data products can provide high spatial resolution and long-term homogeneous  
63 data for previously unmonitored areas at scales that are suitable for studying changes in the  
64 hydrological cycle and for water management applications (Sheffield et al., 2018). Several gridded  
65 data products with global coverage have been produced in recent decades including reanalysis and  
66 satellite-based products. Examples of reanalysis products include Watch Forcing Data applied to  
67 ERA-Interim (Weedon et al., 2014) and Climate Forecast System Reanalysis (Saha et al., 2014).

68 There is also a plethora of satellite products for different hydrometeorological variables such as  
69 precipitation, temperature, soil moisture, and ET. For satellite derived ET estimates, it is worth noting  
70 that this variable cannot be directly measured by satellites, but rather derived from physical variables  
71 observed by satellites from space such as radiation flux. As such, satellite derived ET estimates could  
72 rather be referred to as model outputs constrained by satellite data. Another technique used to produce  
73 ET estimates is the complimentary relationship (Ma et al., 2021). Considering the way gridded ET  
74 products are derived, they tend to suffer from large biases (Weerasinghe et al., 2020; Mcnamara et  
75 al., 2021) and therefore need to be validated before use. In fact, it is argued that validating gridded  
76 ET products is an essential step in understanding their applicability and usefulness in water  
77 management operations (Blatchford et al., 2020).

78 Previously, much attention in the development of gridded environmental data was focused on  
79 hydrometeorological variables such as precipitation and temperature. However, rapid advancement  
80 in computer technology has led to the development of gridded water resources reanalysis (WRR) with  
81 quasi global coverage using both land surface models (LSMs) and Global Hydrological Models  
82 (GHMs) driven by satellite and reanalysis data. Examples of WRR products include the Global Land  
83 Data Assimilation System [GLDAS] (Rodell et al., 2004), “The Global Earth Observation for  
84 Integrated Water Resources Assessment” [earth2Observe] (Schellekens et al., 2017), and the Global  
85 Flood Awareness System [GloFAS-ERA5] (Harrigan et al., 2020). Several studies have demonstrated  
86 that model-based gridded WRR products can be used as an alternative to observe river discharge in  
87 poorly gauged basins to: (1) understand hydrological processes (Koukoula et al., 2020), (2) support  
88 transboundary water management (Sikder et al., 2019), (3) identify flood events (Gründemann et al.,  
89 2018; López et al., 2020), and (4) support national water policies (Rodríguez et al., 2020). These  
90 examples demonstrate that WRR products have great potential for addressing water security  
91 challenges in poorly gauged basins. Despite their numerous advantages, outputs from WRR are also  
92 fraught with uncertainties resulting from errors in the forcing data, model structure, and the  
93 parameterisation of the physical processes in the model scheme (Koukoula et al., 2020). Therefore, it  
94 is necessary to evaluate the performance of these products against observed river discharge where  
95 available.

96 Whilst the use of outputs from WRR in water management has gained significant attention in  
97 many ungauged or poorly gauged regions such as Asia and Latin America (López et al., 2020;  
98 Rodríguez et al., 2020; Sikder et al., 2019), they remain largely under-utilized in Africa. For example,  
99 there are only a few case studies reporting on the use of these products in the Upper Blue Nile River  
100 basin (Koukoula et al., 2020; Lakew et al., 2020) and the Zambezi River basin (Gründemann et al.,  
101 2018). Considering the scale of water insecurity in Africa -compounded by acute data scarcity  
102 (Nkiaka et al., 2021), we feel that evaluating the performance of gridded WRR products in Africa

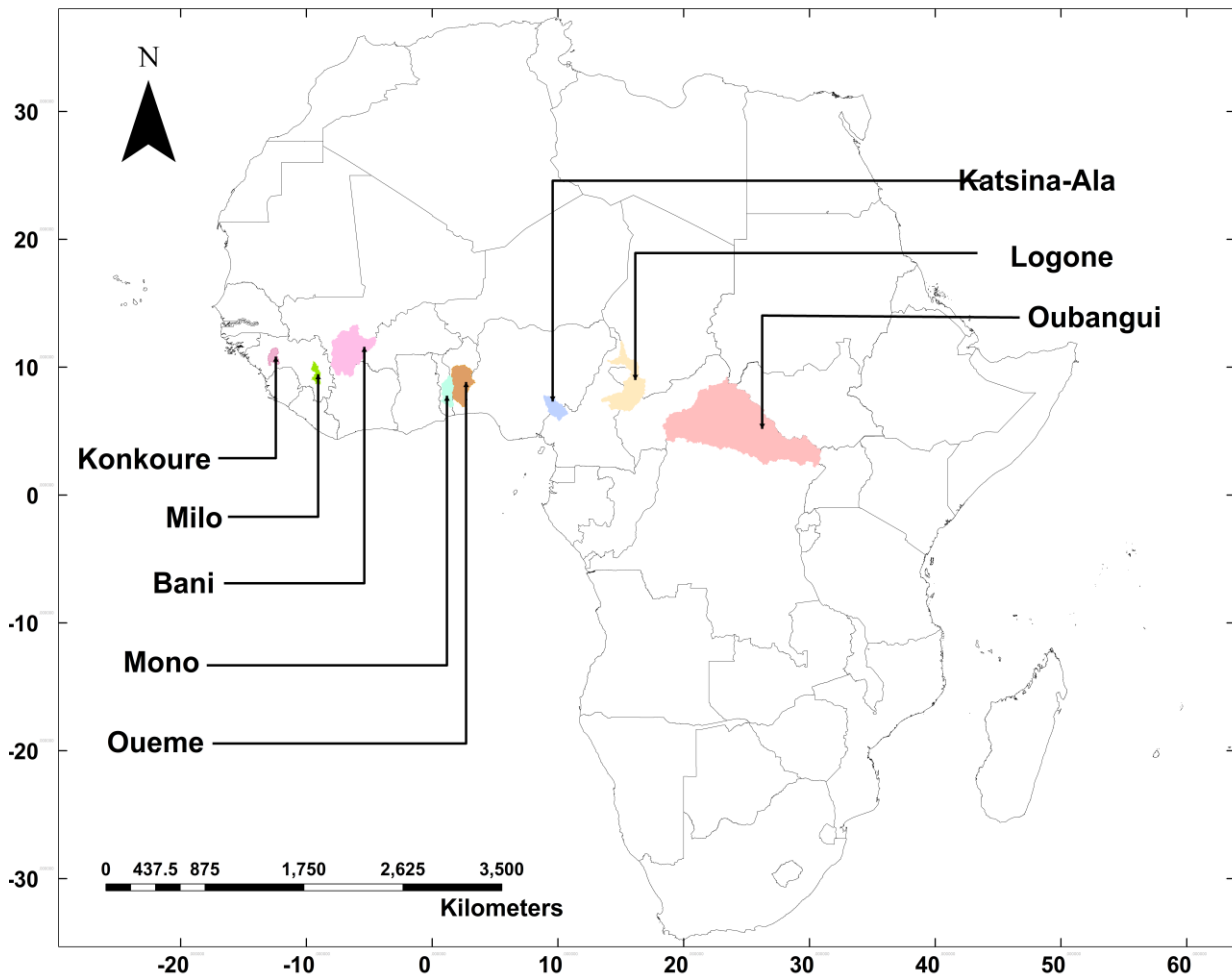
103 may enhance their adoption in water management in the region. On the other hand, several studies  
104 evaluating the performance of gridded data in Africa have focused mostly on precipitation (Dinku et  
105 al., 2018; Satgé et al., 2020) while few studies that have evaluated gridded ET products focused on  
106 large basins, (Blatchford et al., 2020; Weerasinghe et al., 2020; Mcnamara et al., 2021) and mostly  
107 adopting an annual timescale. This may be attributed to the large scale of the basins which is ideal  
108 for the application of satellite data and the coarse spatial resolution of some of the ET products. The  
109 availability of high spatial and temporal resolution ET products suggest that it is now possible to  
110 evaluate these products in small- to medium-size basins and at a higher temporal resolution.

111 The objectives of this paper were to: (1) evaluate the performance of earth2Observe Tier 1  
112 and other WRR products in simulating discharge and evapotranspiration in selected small to medium-  
113 size basins in Central-West Africa, and (2) evaluate the performance of six satellite-based gridded  
114 ET estimates and ET estimates obtained using the complimentary relationship (CR-ET). Considering  
115 that only a few studies have attempted to evaluate gridded WRR and ET products over Africa, this  
116 paper contributes to the contemporary debate on the performance of these products and how there  
117 can be used to assess water security in poorly gauged basins. We evaluated ET estimates from WRR  
118 and other sources considering that users needs for the application of these products may vary. Hence  
119 our evaluation covered a wide range of models and products to align with the needs of different users.

## 120 **2. Materials and methods**

### 121 **2.1. Study area**

122 The selected basins are located in Central-West Africa ranging in size from 9,000 km<sup>2</sup> to 499,000  
123 km<sup>2</sup> (Figure 1). Rainfall in the region is mostly controlled by the north-south movement of the  
124 intertropical convergence zone (ITCZ). The main criteria for selecting the basins were: (1) availability  
125 of observed river discharge data and (2) for the period of the available discharge data to coincide with  
126 the period when gridded WRR and ET data are also available. Model evaluation timestep was  
127 determined by the timestep of river discharge data. Shapefiles for all the basins were obtained from  
128 HydroSHEDS, locations of the discharge gauging stations were obtained from the respective data  
129 sources while the area of each basin was calculated from the basin shapefiles. HydroSHEDS drainage  
130 network offers the unique opportunity to generate watershed boundaries for GRDC gauging stations  
131 using a proofed dataset and applying a consistent methodology. Table 1 shows that some of the basins  
132 are transboundary in nature.



133  
134 **Figure 1:** Locations of the eight river basins where the performance of WRR and gridded ET  
135 products were evaluated

136 **Table 1:** Characteristics of river basins and sources of river discharge data

Basin	Total area (km <sup>2</sup> )	Transboundary (Yes or No) Countr(y/ies)	Population (thousands)	Source of river discharge data
Bani	101,600	(Yes) Ivory Coast, Mali, and Burkina Faso	63,766	GRDC
Katsina-Ala	22,963	(Yes) Cameroon and Nigeria	219,875	NHSA
Konkoure	10,250	(No) Guinea-Conakry	13,053	GRDC
Logone	87,953	(Yes) Cameroon, Chad, and Central Africa Republic	44272	LCBC
Milo	9,620	(No) Guinea-Conakry	13,053	GRDC
Mono	21,575	(Yes) Togo, Benin	21,479	Co-author
Oubangui	499,000	(Yes) Central Africa Republic and the Democratic Republic of Congo	88,742	GRDC
Oueme	46,990	(No) Benin	11,488	Co-author

137 Global River Discharge Centre [GRDC], Nigeria Hydrological Services Agency [NIHSA], Lake Chad Basin Commission  
138 [LCBC]. Population data sourced from (Undesa, 2019)

## 139 2.2. Input data

### 140 2.2.1. Water resources reanalysis (WRR)

141 The WRR product evaluated in this study include “The Global Earth Observation for Integrated Water  
142 Resources Assessment” (earth2Observe), Famine Early Warning Systems Network [FEWS NET]  
143 Land Data Assimilation System (FLDAS), and TerraClimate. The earth2Observe Tier 1 product

144 consists of a multi-model ensemble of ten global models at a spatial resolution of  $0.5^\circ \times 0.5^\circ$  spanning  
 145 from 1979 to 2012 and driven by Watch Forcing Data methodology applied to ERA-Interim  
 146 reanalysis (WFDEI) data (Schellekens et al., 2017). WRR data from earth2Observe are freely  
 147 available at (<https://wci.earth2observe.eu/portal/>). Model evaluation here omits the Joint UK Land  
 148 Environment Simulator (JULES), Simple Water Balance Model (SWBM), and the simple conceptual  
 149 HBV hydrological model (HBV-SIMREG) as data from the models was not available from the portal  
 150 for the selected basins at the time of writing. As such, seven models and a model ensemble were  
 151 included in this study. Evaluation of ET data also omits Lisflood model as data was not available  
 152 from the portal at the time writing. Although there is an available Tier 2 product with a higher spatial  
 153 resolution ( $0.25^\circ$ ), this study did not utilise these data as selected basins were not included at the time  
 154 of conducting this research. We also evaluated discharge data from FLDAS-Noah and TerraClimate  
 155 with spatial resolutions of  $0.1^\circ$  and  $0.041^\circ$  respectively. Table 2 provides a brief summary of the  
 156 different models used in this study.

157 **Table 2:** Water resources reanalysis (WRR) products evaluated

Model provider	Model name	Model type	Routing scheme	Reference
CNRS (Centre National de la Recherche Scientifique)	ORCHIDEE (Organizing Carbon and Hydrology in Dynamic Ecosystems)	LSM	Cascade of linear reservoirs	(Krinner et al., 2005)
CSIRO (Commonwealth Scientific and Industrial Research Organization)	AWRA-L (Australian Water Resources Assessment)	GHM	Cascade of linear reservoirs	(Van Dijk et al., 2014)
ECMWF (European Centre for Medium-Range Weather Forecasts)	HTESEL (Hydrology Tiled ECMWF Scheme for Surface Exchanges over Land)	LSM	CaMa-Flood	(Balsamo et al., 2009)
JRC (Joint Research Centre)	LISFLOOD	GHM	Double kinematic wave	(Van Der Knijff et al., 2010)
UniUt (Universiteit Utrecht)	PCR-GLOBWB	GHM	Travel time	(Van Beek et al., 2011)
MeteoFr (Meteo France)	SURFEX	LSM	TRIP with stream	(Decharme et al., 2010)
UniK (Universitat Kassel)	WaterGAP	GHM	Manning–Strickler	(Wada et al., 2014)
NASA	FLDAS-Noah	LSM	Soil-layer water and energy balance	(McNally et al., 2017)
University of California Merced	TerraClimate	GHM	Bucket type model	(Abatzoglou et al., 2018)

158

### 159 2.2.2. Evapotranspiration products

160 In addition to the ET estimates from the reanalysis products, we also evaluated several satellite-based  
 161 ET estimates including GLEAM3.5a & 3.5b, MODIS16A2, PMLV1, PMLV2, SSEBop and estimates  
 162 obtained through complimentary relationship (Table 3). ET products from WRR have the same spatial  
 163 resolution with the discharge estimates while remote sensing products have different spatial

164 resolutions. However, we did not resample the ET data to the same resolution because a previous  
 165 study has shown that resampling does not have any significant impact on the results (Weerasinghe et  
 166 al., 2020). Table 3 provides a summary of all ET products evaluated in this study.

167 **Table 3: Characteristics of the different ET products**

ET product	Core equation	Temporal resolution	Spatial resolution	References
GLEAM3.5a & 3.5b	Priestley-Taylor	Monthly	0.25° x 0.25°	(Martens et al., 2017)
MODIS16A2	Penman-Montieth	8-day	1/48°x1/48°	(Mu et al., 2007; Mu et al., 2011)
PMLV1	Penman-Monteith-Leuning	Monthly	0.5° x 0.5°	(Zhang et al., 2016)
PMLV2	Penman-Monteith-Leuning	8-day	1/192°x1/192°	(Zhang et al., 2019)
SSEBop	Surface Energy Balance	Monthly	1/96° x 1/96°	(Senay et al., 2013)
CR-ET	Penman-Montieth	Monthly	0.25°	(Ma et al., 2021)

168

## 169 2.3. Evaluation data

169

### 170 2.3.1. River discharge

170

171 Observed river discharge data were used to evaluate the performance of WRR models and to estimate  
 172 basin-wide water balance evapotranspiration ( $ET_{WB}$ ) using the water balance concept. The source of  
 173 the river discharge data is available in Table 1. Gaps in the discharge data were filled using Self-  
 174 Organizing Maps which which is a robust method for infilling missing gaps in hydrometeorological  
 175 time series (Nkiaka et al., 2016).

176

### 176 2.3.2. Precipitation

177 Precipitation data were to estimate basin-wide water balance evapotranspiration ( $ET_{WB}$ ). To reduce  
 178 uncertainties inherent in precipitation estimates, an ensemble mean of three different satellite-based  
 179 precipitation products was used. The different products were Climate Hazards Group InfraRed  
 180 Precipitation with Station data [CHIRPS] (Funk et al., 2015), Precipitation Estimation from Remotely  
 181 Sensed Information using Artificial Neural Networks-Climate Data Record [PERSIANN-CDR]  
 182 (Ashouri et al., 2015) and Global Precipitation measurement [GPM] (Skofronick-Jackson et al.,  
 183 2018). The precipitation products have spatial resolutions of 0.05°, 0.1° and 0.25° for CHIRPS, GPM  
 184 and PERSIANN-CDR respectively. These precipitation products have been validated extensively  
 185 across the study domain (Satgé et al., 2020; Dembélé et al., 2020) and used in several studies in Africa  
 186 (Larbi et al., 2021; Nkiaka, 2022). The data were downloaded as the spatial average for each basin  
 187 using the Climate Engine research App.

188

### 188 2.3.3. GRACE

189 GRACE data are monthly anomalies of terrestrial water storage changes (TWSC) used to quantify  
 190 changes in terrestrial water storage. The dataset has a global coverage spanning the period 2003–2017

191 (Tapley et al., 2019). The data has a coastline resolution improvement (CRI) filter to reduce leakage  
192 errors across coastlines and land-grids, using scaling factors derived from the community land model  
193 (Wiese et al., 2016). The data has recently been re-processed to reduce measurement errors and  
194 represents a new generation of gravity solutions that do not require empirical post-processing to  
195 remove correlated errors, as such, the present data is better than the previous GRACE version that  
196 was based on spherical harmonic gravity solution (Wiese et al., 2016). To minimize errors and  
197 uncertainties in the GRACE-derived TWSC estimates, we used an ensemble mean of three GRACE  
198 mascon solutions derived from different processing centres including Jet Propulsion Laboratory (JPL)  
199 RL06M Version 2.0 GRACE mascon solution with a spatial resolution of  $0.5^\circ \times 0.5^\circ$ , Center for  
200 Space Research at University of Texas, Austin (CSR GRACE/GRACE-FO RL06 v02 Mascon Grids)  
201 with a spatial resolution of  $0.25^\circ \times 0.25^\circ$  and NASA GSFC GRACE and GRACE-FO MASCON  
202 RL06 v1.0 with spatial resolution of  $0.5^\circ \times 0.5^\circ$ . GRACE data were used to estimate basin-wide water  
203 balance evapotranspiration ( $ET_{WB}$ ).

#### 204 **2.4. Evaluating gridded WRR**

205 WRR models were evaluated following a multi-objective approach commonly used in evaluating the  
206 performance of hydrological models, including the Nash-Sutcliffe efficiency (NSE), Kling-Gupta  
207 efficiency (KGE), and the percent bias (PBIAS). NSE scores range from  $-\infty$  to 1, with 1 indicating a  
208 perfect representation of observed discharge. NSE scores  $\geq 0.50$  can be considered acceptable whereas  
209 NSE scores  $\leq 0.0$  indicate poor model performance (Moriasi et al., 2007). Similarly, the KGE is a  
210 dimensionless metric that can be decomposed into three components crucial for evaluating  
211 hydrological model performance accounting for temporal dynamics (correlation), bias errors  
212 (observed vs simulated volumes), and variability errors (relative dispersion between observations and  
213 simulations) (Gupta et al., 2009). KGE scores range from  $-\infty$  to 1, with 1 considered the ideal value.  
214 Next, PBIAS is used to measure the tendency of the simulated discharge to be larger or smaller than  
215 their observed counterparts (Gupta et al., 2009). PBIAS is expected to be 0.0, with low magnitude  
216 values indicating accurate simulations, positive values indicate underestimation, negative values  
217 indicate overestimation (Moriasi et al., 2007). According to Moriasi et al. (2007), a hydrological  
218 model with PBIAS values in the range  $\pm 25\%$  can be considered to be acceptable. Furthermore, a  
219 temporal evaluation of flow hydrographs was carried out by plotting the monthly simulated vs  
220 observed discharge to ascertain visually if the models were able to capture the magnitude, seasonality,  
221 and interannual variability of discharge.

222

223

224 **Table 4: Contingency table for 80<sup>th</sup> percentile river discharge**

	Observed discharge		
		Yes	No
Simulated discharge	Yes	Hits (H)	False Alarms (FA)
	No	Misses (M)	Correct Negatives

225

226 Lastly, we evaluated the models ability to predict discharge above specific thresholds. This evaluation  
 227 step is of critical importance when considering operational water management requirements such as  
 228 water allocation and reservoir operation which rely on monthly river discharge. To achieve this, we  
 229 adopted the Critical Success Index (CSI) as the metric to evaluate the ability of each model to simulate  
 230 discharge at 20<sup>th</sup> and 80<sup>th</sup> percentiles (i.e. discharge at 80<sup>th</sup> and 20<sup>th</sup> percent exceedance respectively).  
 231 CSI is calculated from a two-dimensional contingency table defining the events in which observed  
 232 and simulated discharges exceed a given threshold (Thiemig et al., 2015). We used the 20<sup>th</sup> and 80<sup>th</sup>  
 233 percentiles to assess the ability of the models to simulate both low and high flows respectively. The  
 234 contingency table (Table 4) is a performance measure used in summarizing all possible forecast-  
 235 observation combinations such as hits (H; event forecasted and observed), misses (M; event observed  
 236 but not forecasted), false alarms (FA; event forecasted but not observed) and correct negatives (CN;  
 237 event neither forecasted nor observed). The ideal value for CSI is 100% and the metric is calculated  
 238 as follows:

239 
$$CSI = \frac{H}{H + M + FA} \times 100 \quad (1)$$

240 **2.5. Evaluating gridded ET**

241 We also adopted a multi-step approach to evaluate the performance of ET products by assessing the  
 242 annual ET–precipitation ratio, evaluating the statistical performance of ET products against long-term  
 243  $ET_{WB}$  and the ability of the products to capture monthly ET variability.

244 In the first step, the annual ET–precipitation ratio was calculated to compare with the ratio  
 245 obtained using  $ET_{WB}$  method. The ET–precipitation ratio can also provide an estimate of the amount  
 246 of water available in each basin after evapotranspiration losses. In the second step, different statistical  
 247 metrics were used to assess the performance of the ET products using the monthly  $ET_{WB}$  as a reference  
 248 (Andam-Akorful et al., 2015; Koukoula et al., 2020). The monthly  $ET_{BW}$  was calculated using the  
 249 basin water balance equation as follows:

250 
$$ET_{WB} = P - Q - \Delta S \quad (2)$$

251 Where  $P$  is average monthly precipitation over the basin (mm),  $Q$  is river discharge (mm) and  $\Delta S$  is  
 252 the terrestrial water storage change [TWSC] (mm). Unlike several studies that have evaluated ET  
 253 products on an annual timescale, this study adopts a monthly sample. As such, the TWSC component

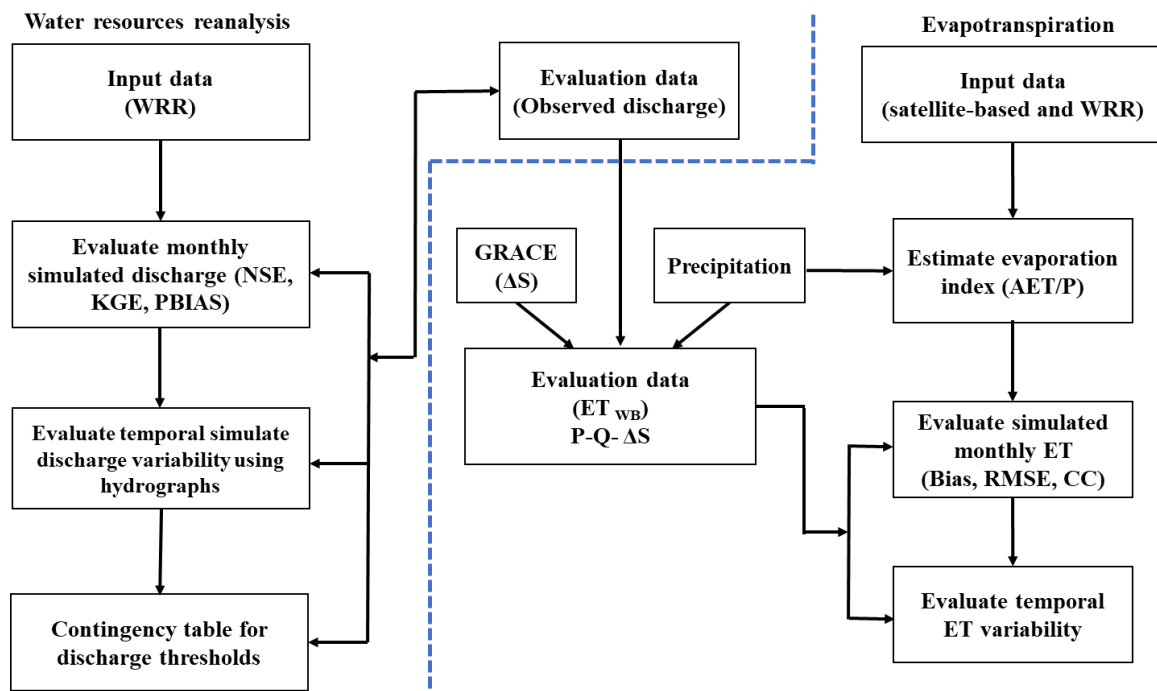
254 ( $\Delta S$ ) in equation 2 that is often neglected when estimating  $ET_{WB}$  over several years ( $\geq 10$  years) could  
255 not be overlooked. Due to the likely impact of anthropogenic activities such as reservoir operation,  
256 water withdrawal, and monthly rainfall variability on TWSC, values derived at monthly timescales  
257 are important. TWSC data used in this study were the mean of three different GRACE mascon  
258 solutions produced by different processing centres highlighted earlier.

259 Due to its coarse spatial resolution, it has been argued that GRACE is not sensitive at detecting  
260 changes in monthly TWSC in small-size basins  $\leq 150,000 \text{ km}^2$  (Rodell et al., 2011). Based on this  
261 claim, it might be argued that GRACE data may not be applicable in this study considering that most  
262 of the basins are below this threshold except the Oubangui ( $499,000 \text{ km}^2$ ). However, several studies  
263 (Liu, 2018; Biancamaria et al., 2019; Oussou et al., 2022; Xie et al., 2022), have demonstrated that  
264 GRACE can provide acceptable TWSC estimates for basins that are smaller than this threshold. To  
265 further minimize errors and uncertainty in the GRACE-derived TWSC in our smaller-size basins, we  
266 re-gridded the GRACE mascon solutions from JPL and NASA to a spatial resolution of  $0.25^\circ$  which  
267 is the same spatial resolution for the mascon solutions from CSR. We then proceeded to extract and  
268 average the timeseries of all coincident GRACE grid cells for each basin from the three different  
269 mascon solutions with the same spatial resolution. Gaps in the time series were infilled using the  
270 linear function in Python. Finally, we calculated the ensemble mean of the three solutions to represent  
271 GRACE-derived TWSC estimate for each basin. To estimate changes in monthly TWSC, we  
272 calculated the difference between consecutive GRACE measurements for each basin, divided by the  
273 time between measurements, using the following equation:

$$274 \quad \Delta S = (S_{[n]} - S_{[n-1]})/dt \quad (3)$$

275 Where  $\Delta S$  represents the TWSC (mm),  $n$  is the measurement number, and  $dt$  is the time difference  
276 between two consecutive GRACE measurements (months).

277 Lastly, temporal evaluation of the products was carried out by plotting the time series of all  
278 ET products against  $ET_{WB}$  to visually establish if the gridded ET products were able to capture the  
279 magnitude, seasonality, and interannual variability of ET across the basins.



280

281

282

**Figure 2:** Flowchart outlining the steps used in evaluating the WRR and ET products (The blue dotted line in the flow chart separates evaluation of WRR from ET products)

283

### 3. Results

284

#### 3.1. Water resources reanalysis products

285

##### 3.1.1. Hydrological performance

286

287

288

289

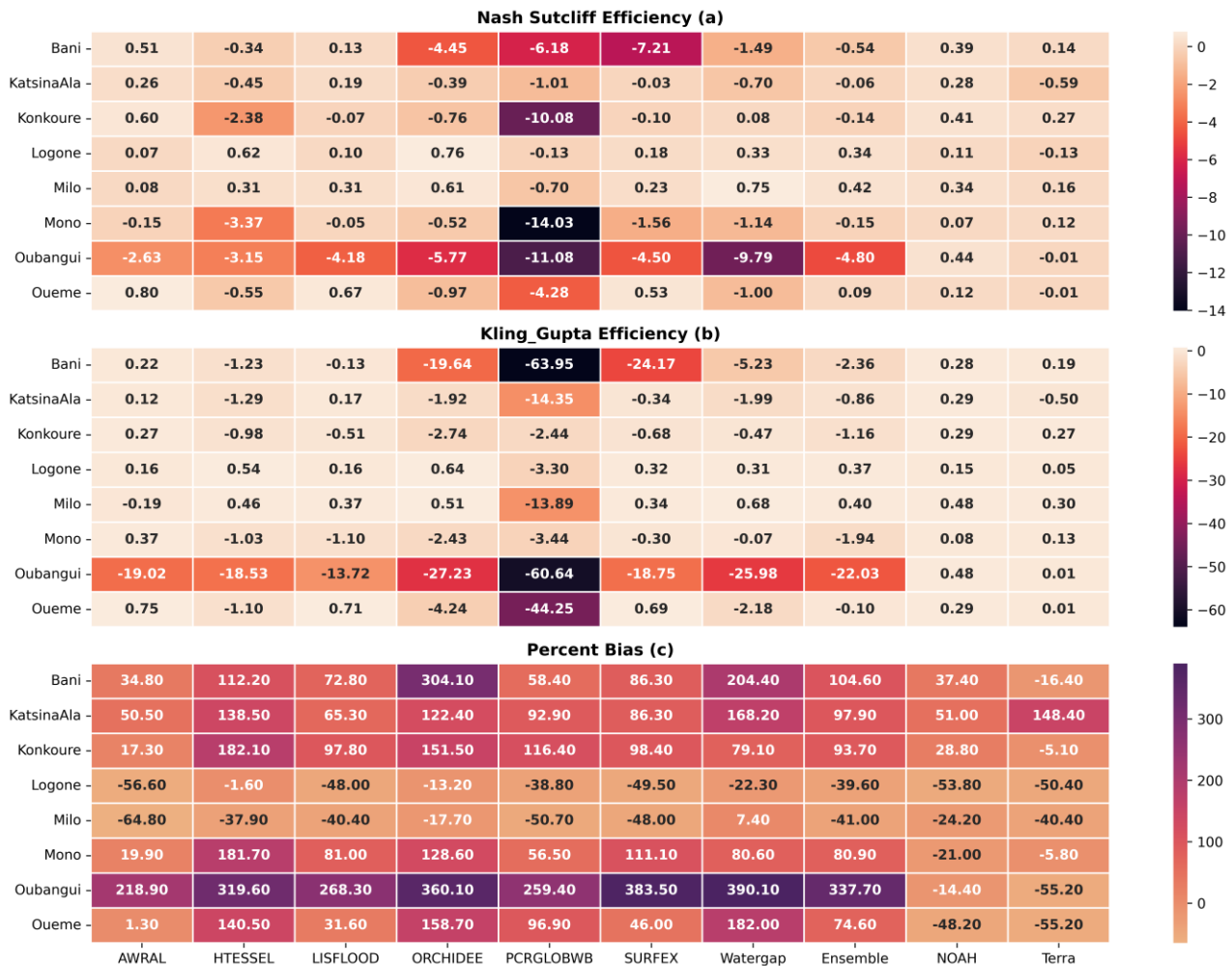
290

291

292

293

A multi-objective approach using different statistical metrics (NSE, KGE and PBIAS) was used to evaluate discharge estimates from WRR products. The performance of the models in simulating discharge is shown in Figure 3. Using the NSE as a performance metric, results show that FLDAS-Noah produced positive scores in all the basins (0.15–0.48). Terra, AWRAL and Lisflood produced positive scores (0.01–0.75) in seven, six and four basins respectively. SURFEX model produced positive scores in three basins while ORCHIDEE, HTESSSEL, Watergap and the ensemble mean produced positive scores in two basins each while PCR-GLOBW produced negative scores in all the basins (Figure 3a).



294

295 **Figure 3:** Statistical evaluation of the models using (a) NSE, (b) KGE, and (c) PBIAS. Red and  
 296 orange colours represent poor model performance in Figures 3a, 3b & 3c, however, the acceptable  
 297 PBIAS range in Figure 3c is  $\pm 25\%$ . Ensemble refers to the mean of WRR from the earthH2Observe.

298 KGE results show that FLDAS-Noah also produced positive scores (0.11– 0.44) in all basins,  
 299 followed by AWRAL, Lisflood and Terra with positive scores in six, five and four basins respectively  
 300 (Figure 3b). SURFEX and Watergap produced positive scores in three basins while ORCHIDEE and  
 301 HTESSEL produced positive scores (0.31–0.76) in two basins. The ensemble mean produced positive  
 302 scores (0.09 – 0.42) in three basins while PCRGLOBWB produced the lowest KGE scores (Figure 3b).

303 Positive and negative PBIAS values were obtained in the different basins. Negative values  
 304 indicate that the model overestimated discharge volumes compared to observed discharge while  
 305 positive values indicate the opposite. FLDAS-Noah, Terra and AWRAL produced acceptable PBIAS  
 306 scores ( $\pm 25\%$ ) in three basins, ORCHIDEE and Watergap produced similar scores in two basins and  
 307 HTESSEL in one basin (Figure 3c). The rest of the models including the ensemble mean either grossly  
 308 overestimated or underestimated discharge volumes in all the basins.

309

310

311

### 3.1.2. Temporal evaluation

312

313

314

315

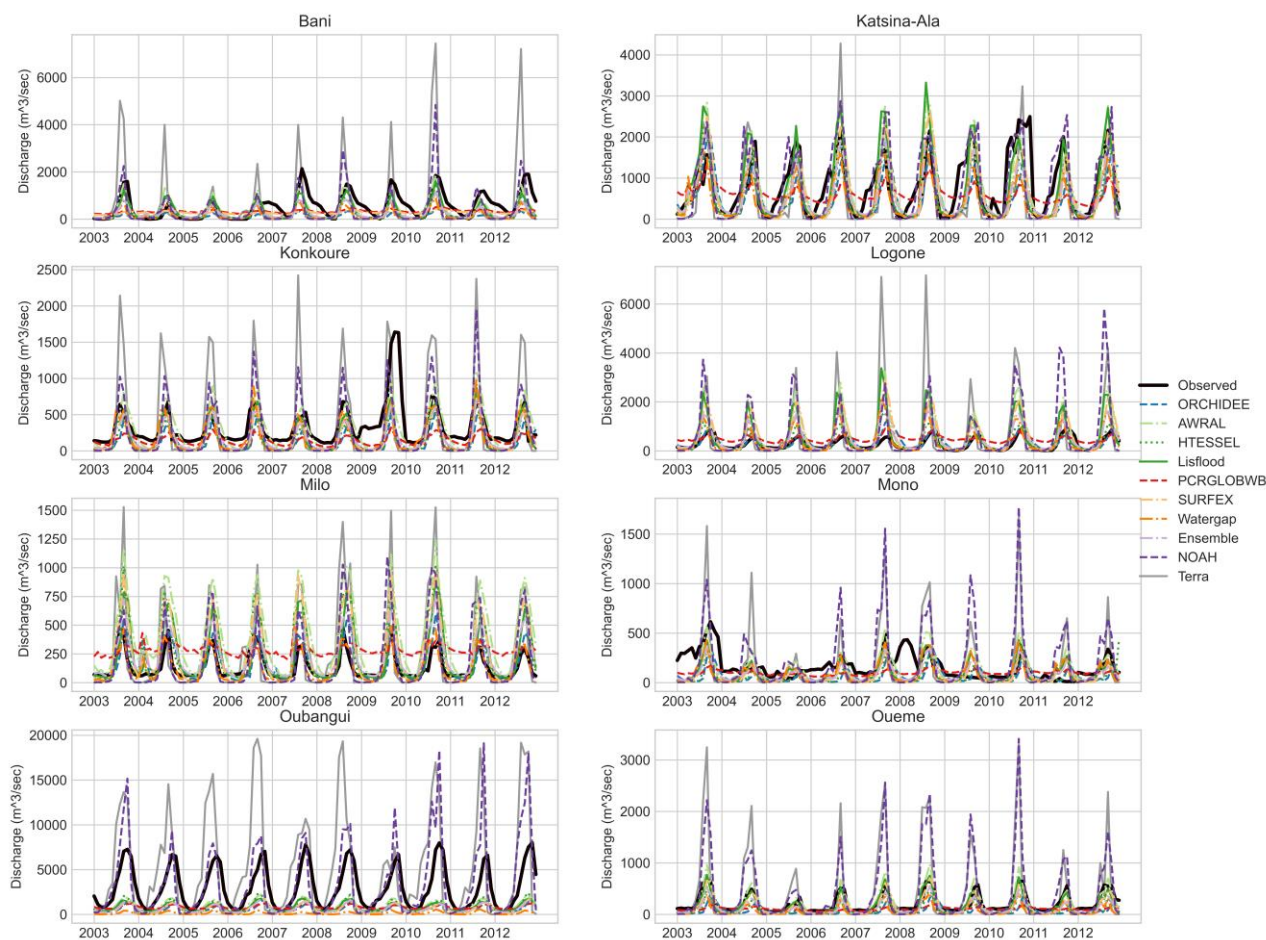
316

317

318

319

The ability of the models to capture discharge variability was analysed by comparing the simulated vs observed discharge. Results show that most of the models were able to capture the seasonal discharge variability including peak and low flows (Figure 4). However, PCR-GLOBW systematically overestimated low flows and underestimated high flows across all basins. In the Oubangui basin, all models were able to capture the seasonal variability but consistently underestimated peak flows except FLDAS-Noah and Terra models which both overestimated peak flows (Figure 4). For example, measured peak discharge in the river exceeds 5000 m<sup>3</sup>/sec, but all models except FLDAS-Noah and Terra simulated it to be less than 2000 m<sup>3</sup>/sec (Figure 4).



320

321 **Figure 4:** Evaluation of temporal flow variability simulated by the different model

322

### 3.1.3. Critical Success Index

323

324

325

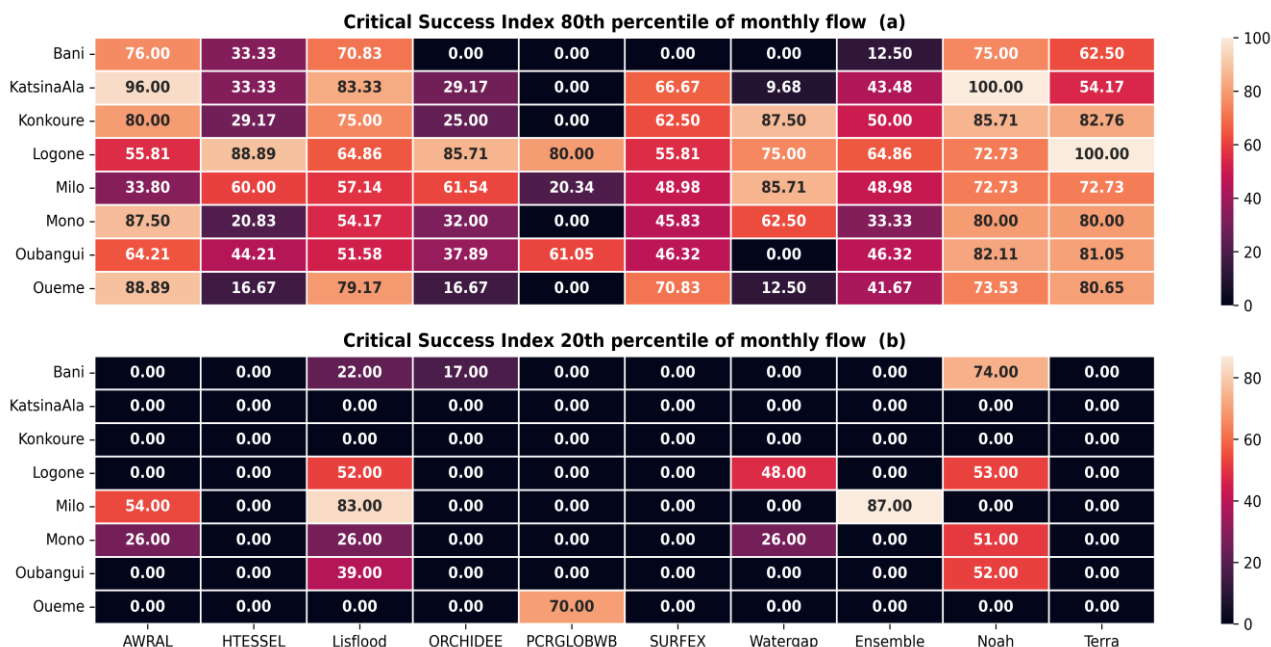
326

327

328

Figure 5 shows the performance of the models in simulating the 80<sup>th</sup> and 20<sup>th</sup> percentiles monthly discharge. For the 80<sup>th</sup> percentile flows, results show that FLDAS-Noah and Terra produced CSI scores above 50 % in all basins followed by Lisflood and AWRAL in seven and six basins respectively while Surfex and Watergap produced similar scores in four basins each (Figure 5a). For the 20<sup>th</sup> percentile flows, only FLDAS-Noah produced CSI scores above 50 % in four basins while Lisflood produced similar scores in two basins. The performance of the other models in simulating

329 the 80<sup>th</sup> percentile flow shows a large spread while most models including the ensemble mean failed  
 330 to simulate the 20<sup>th</sup> percentile flow across all the basins. Taking together, results suggest that the  
 331 models simulated high flows better than the low flows with only FLDAS-Noah capable of capturing  
 332 both flow regimes in most basins (Figure 5b).



333 **Figure 5:** Critical Success Index for 80<sup>th</sup> and 20<sup>th</sup> percentile of monthly flow across all basins

### 335 3.2. Evapotranspiration products

336 Mean monthly Precipitation and GRACE estimates obtained by averaging the three different  
 337 precipitation products and GRACE mascon solutions processed by three different centres are  
 338 available in the supplementary material. The mean of the different products was used in order to  
 339 reduce the uncertainties estimates from a single source are used. The mean precipitation and GRACE  
 340 estimates were used in this study to evaluate the performance of the different evapotranspiration  
 341 products in this study.

#### 342 3.2.1. Evapotranspiration–precipitation ratio

343 Figure 6 shows the annual ET–precipitation ratio for all basins. It can be observed that average annual  
 344 ET–precipitation ratio ranges between (0.56–0.77) for WRR and (0.53–0.83) for satellite-based  
 345 products over a period 2003–2012 across all basins. WaterGap produced the highest ratio (0.46-0.99)  
 346 among WRR models, SSEBop produced the highest ratio (0.54–0.99) while MOD16A2 produced the  
 347 lowest ratio (0.43–0.67) among the satellite-based products (Figure 6). Results show that the  
 348 evaporation ratios from the different ET estimates were mostly in the same order of magnitude with  
 349 the ratio from ET<sub>WB</sub> across all the basins except for WaterGap, SSEBop, MOD16A2 and CR-ET  
 350 which produced values which were beyond this range (Figure 6).

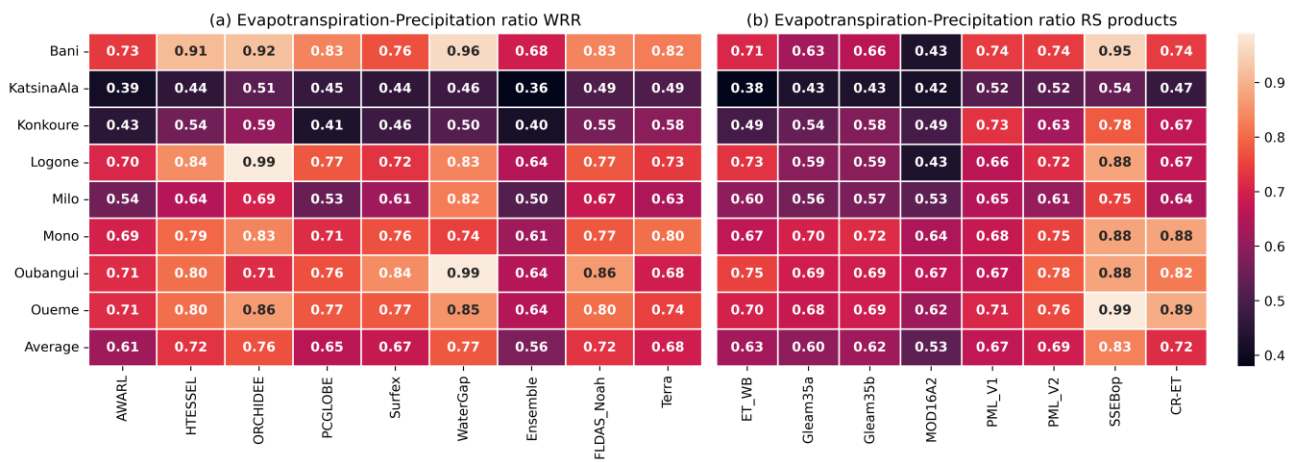


**Figure 6:** Annual evapotranspiration – precipitation ratio 2003 – 2012. WRR: water resources reanalysis and RS: remote sensing

### 3.2.2. Basin-wide water balance estimates

351

352

353

354

355

356

357

358

359

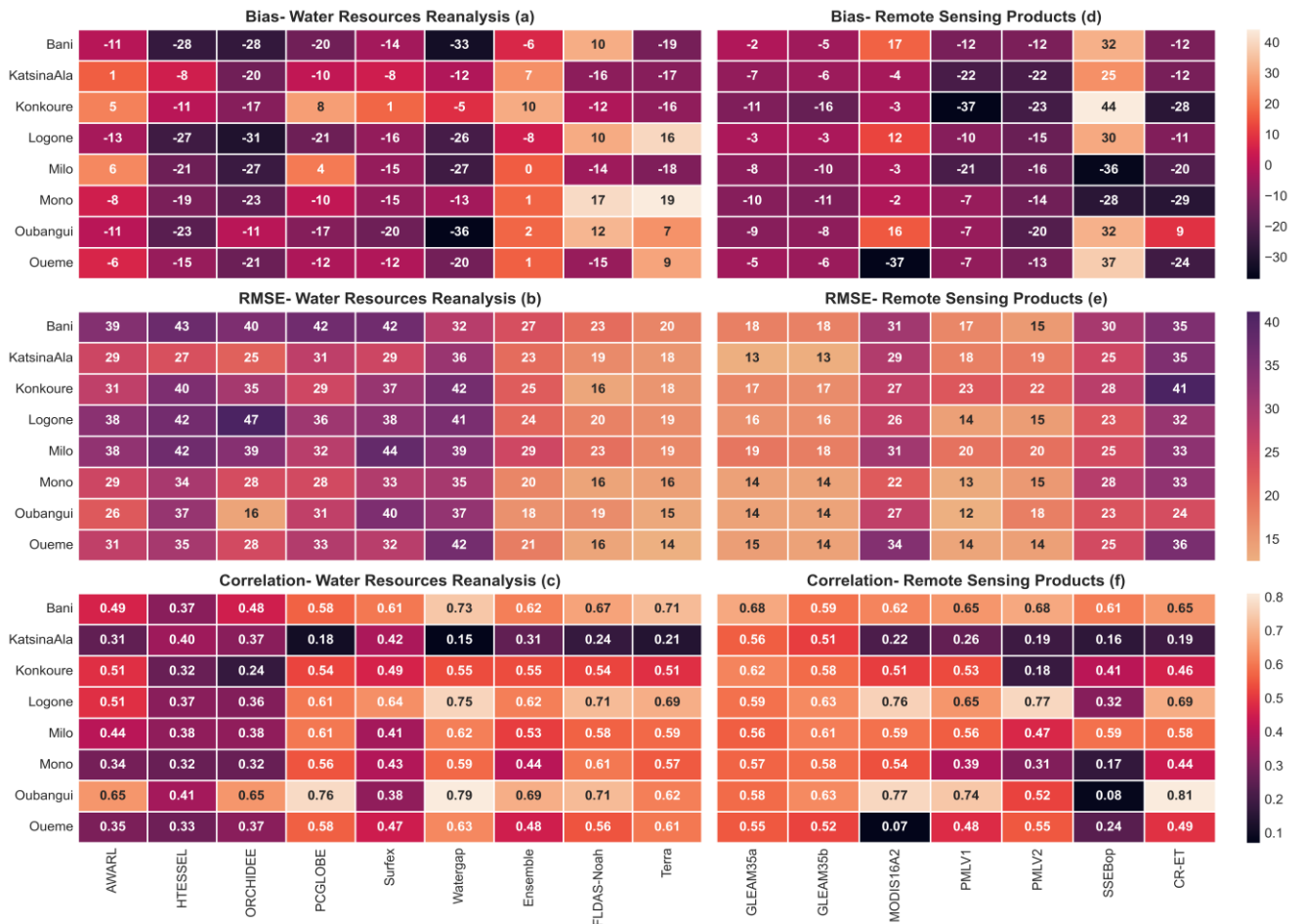
360

361

362

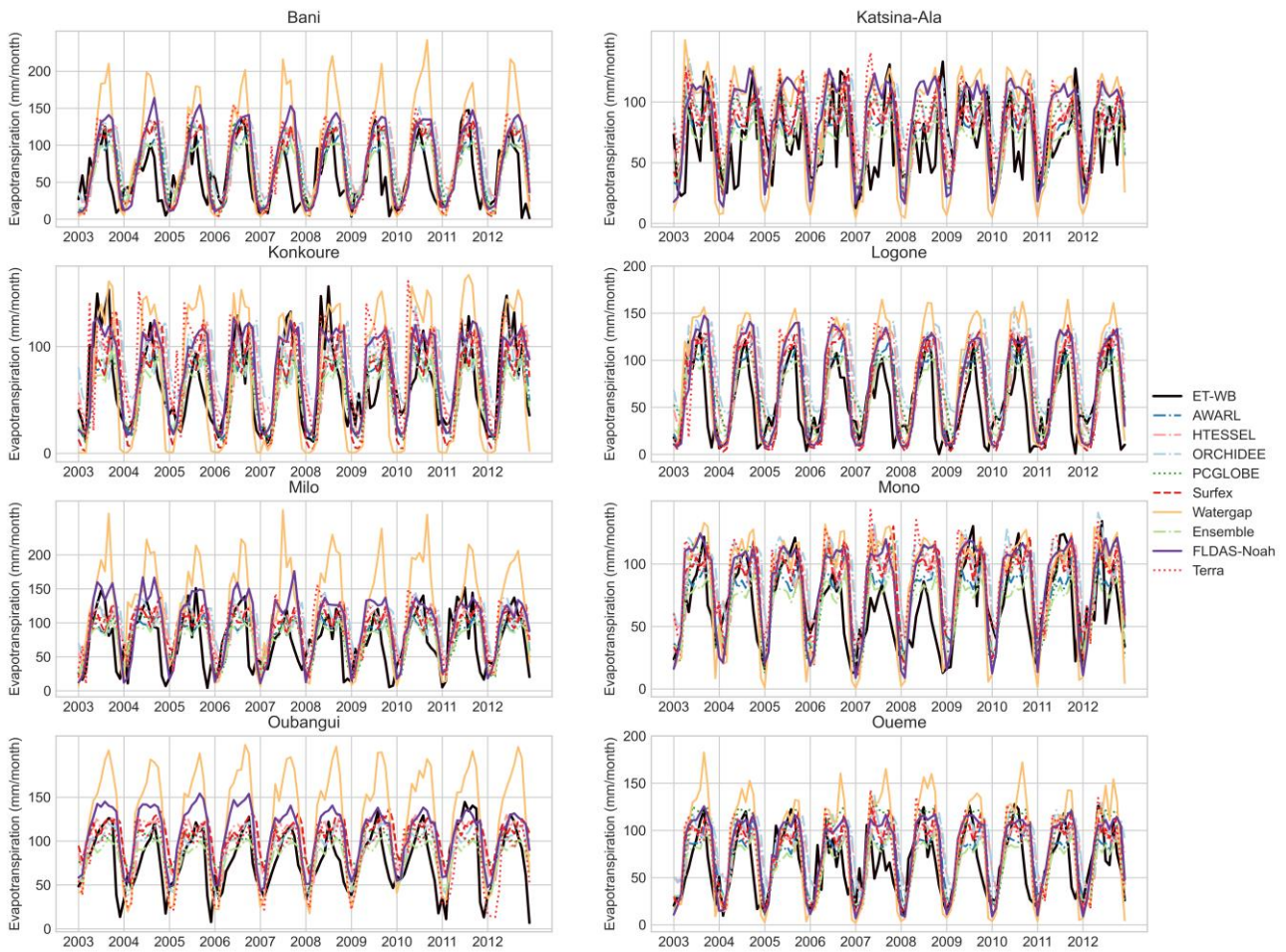
363

Figure 7 shows the results of the statistical metrics used in evaluating the ET estimates using monthly  $ET_{WB}$  as reference. Considering bias as a performance metric, AWARL, FLDAS-Noah and Terra produced the lowest bias scores among WRR products while PMLV2, Terra, and GLEAM3.5a & 3.5b produced the lowest bias scores among the satellite-based products (Figure 7a&d). Most WRR products underestimated ET and similarly most satellite-based products also systematically underestimated ET with among the satellite-based products while the rest of the products produced mixed results (Figure 7a&d). However, SSEBop systematically overestimated ET in all the basins while MOD16A2 grossly underestimated this variable in all but one basin with respect to monthly  $ET_{WB}$  (Figure 7d).



**Figure 7: Bias, RMSE, and Pearson correlation coefficient between monthly  $ET_{WB}$  and different ET products (a-c: WRR and d-f: remote sensing products).**

364  
 365  
 366  
 367 FLDAS-Noah and Terra produced the lowest RMSE (14–23 mm/month) among the WRR products  
 368 while GLEAM3.5a & b and PMLV1 & 2 produced the lowest RMSE (13–23 mm/month) among the  
 369 satellite-based products (Figure 7b&e). The rest of the products both WRR and satellite-based  
 370 produced substantially higher RMSE scores (Figure 7b&e). Among WRR products, only FLDAS-  
 371 Noah and Terra produced slightly higher Pearson correlation scores across most basins (Figure 7c).  
 372 On the other hand most satellite-based products produced high Pearson correlation scores ( $\geq 0.50$ ) in  
 373 all basins except PMLV2 and SSEBop which both produced low scores ( $< 0.50$ ) in four and six basins  
 374 respectively (Figure 7f). ET estimates produced from complimentary relationship (CR-ET)  
 375 performed poorly across most basins.



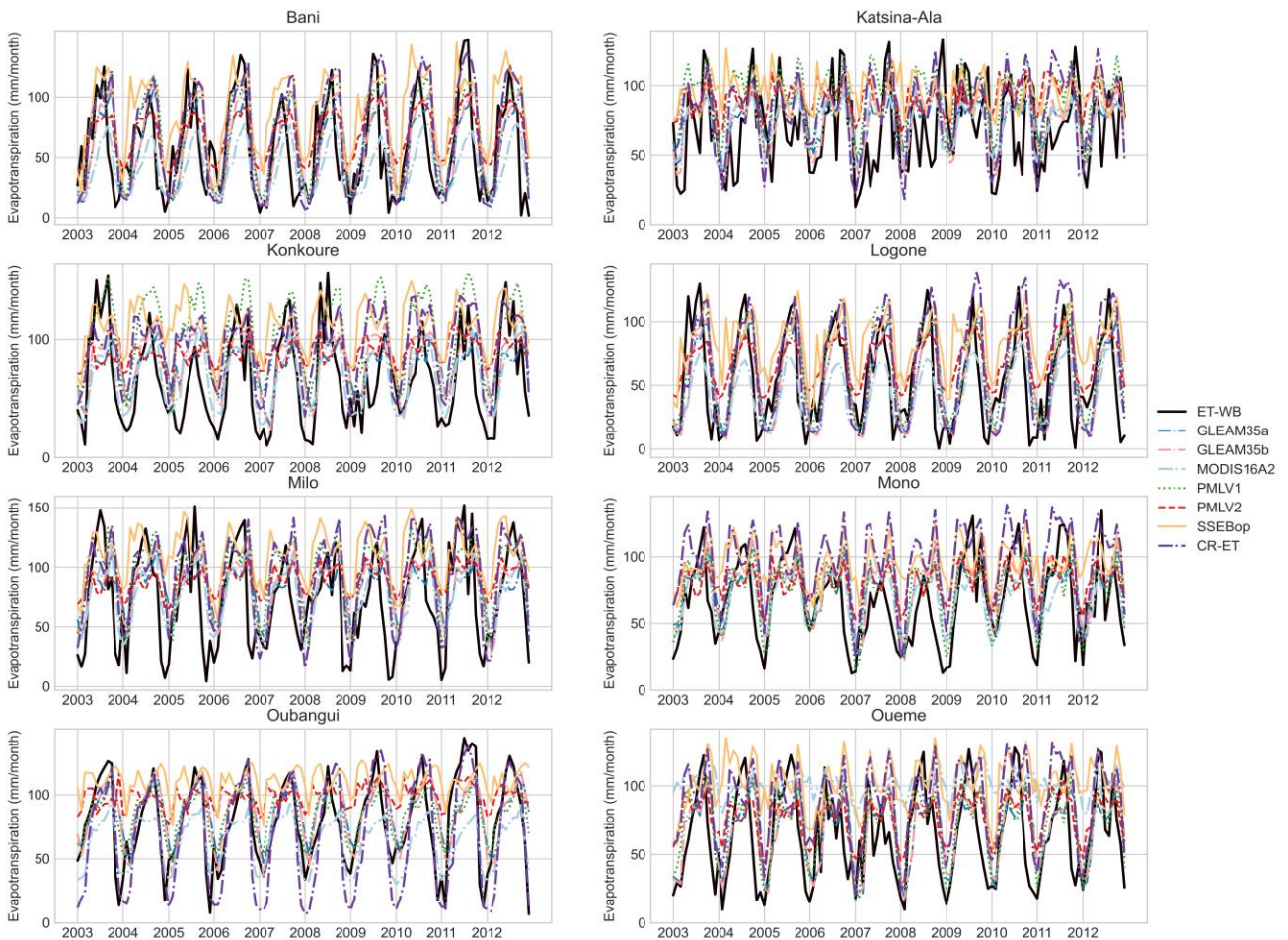
376

377

378

379

**Figure 8a:** Seasonal cycle of ET estimates from WRR and basin-wide water balance evapotranspiration. ET<sub>WB</sub> represents monthly evapotranspiration estimated by the water balance method, while the rest are derived from LSMs and GHMs.



380

381 **Figure 8b:** Seasonal cycle of ET estimates from remote sensing-based products and basin-wide water  
 382 balance evapotranspiration.

383

384

### 3.2.3. Monthly ET variability

385

386 Figure 8 shows the seasonal cycle of  $ET_{WB}$  against both WRR products and satellite-based ET  
 387 estimates. It can be observed that most products were able to replicate the seasonal ET cycle across  
 388 all the basins (Figure 8a&b). Watergap systematically overestimated ET estimates across the all the  
 389 basins among all the WRR products (Figure 8a). SSEBop overestimated ET in some basins among  
 390 the satellite-based products (Figure 8b). The performance of CR-ET follows that of the rest of the  
 products with cases of ET estimate over- and underestimation in some basins.

391

## 4. Discussion

392

393 The overarching goal of this paper was to assess the performance of gridded WRR and ET products  
 394 and to estimate the relative uncertainty in monthly basin-wide evapotranspiration ( $ET_{WB}$ ) estimates.  
 395 Below we provide a discussion and implications of our results in water security assessment in poorly  
 gauged basins.

396

397

#### 398 **4.1. Water resources reanalysis**

399 The performance of WRR products was assessed through commonly used model evaluation metrics,  
400 discharge variability, and verification skill scores (critical success index) using observed river  
401 discharge data. Our results show strong differences in the performance of the different models in  
402 simulating river discharge across the basins. FLDAS-Noah model produced positive NSE and KGE  
403 values in all basins and PBIAS values within the acceptable range ( $\pm 25\%$ ) in three basins. Temporal  
404 evaluation of the WRR products showed that FLDAS-Noah, Terra, AWRAL and Lisflood were able  
405 to capture the seasonal variability in discharge as demonstrated by high KGE scores. Indeed, high  
406 KGE values suggest that some models were able to capture the temporal dynamics (strong  
407 correlation), and low bias scores indicate that the variability errors between the observed discharge  
408 and simulation were also low (Gupta et al., 2009). Nevertheless, Terra consistently overestimated  
409 peak flows in all the basins.

410 Apart from Noah which is a LSM used in FLDAS, most GHMs used in earthH2Observe tier  
411 1 product performed better than the LSMs, which is consistent with results from other studies (Lakew  
412 et al., 2020). The strong performance of GHMs compared to LSMs can be attributed to the differences  
413 in the model structure and parametrisation schemes between LSMs and GHMs (Gründemann et al.,  
414 2018; Koukoula et al., 2020). For example, some GHMs such as Watergap are able to simulate lakes  
415 and reservoirs and water withdrawal while LSMs can only simulate natural processes. Such  
416 differences in model structure can significantly influence discharge volumes simulated by both types  
417 of models (Gründemann et al., 2018). Although PCRGLOBW is a GHM, it produced substantially  
418 low performance compared to the LSMs which is consistent with results from other studies in the  
419 region (Gründemann et al., 2018; Lakew et al., 2020). This suggest that PCRGLOBW model may  
420 not be suitable for assessing water security in the region.

421 The ability of the models to simulate flow thresholds was evaluated using the CSI. Results  
422 show that FLDAS-Noah, Terra, AWRAL and Lisflood were able to capture more than 50% of 80<sup>th</sup>  
423 percentile monthly flow in most basins. We also noted that apart from FLDAS-Noah, the rest of the  
424 GHMs performed better than the LSMs from earthH2Observe in their ability to capture the 80<sup>th</sup>  
425 percentile monthly flows across the basins while only FLDAS-Noah was able to capture 20<sup>th</sup>  
426 percentile flows in three basins. The performance of FLDAS-Noah compared to other models can be  
427 attributed to the fact that it was specially designed and optimized to produce physically meaningful  
428 variables for monitoring food and water security in data-scarce regions in Africa (Mcnally et al.,  
429 2017). Furthermore, FLDAS-Noah and Terra with spatial resolutions of  $0.1^\circ$  &  $0.041^\circ$  respectively  
430 perform better than other models which may be attributed to their higher spatial resolutions compared  
431 to other models with a coarser resolution ( $0.5^\circ$ ). In fact, Gründemann et al. (2018), reported that WRR  
432 products with higher spatial resolution perform better than products with coarser resolution in their

433 ability to simulate discharge. The performance of FLDAS-Noah can also be attributed to the fact the  
434 FLDAS is driven by a combination of different precipitation products thereby reducing the  
435 uncertainty in the input data while earth2observe tier 1 product are driven by one data source (WFDEI)  
436 which increases the uncertainty in the input data which is propagated to the model outputs. Our results  
437 also showed that Lisflood performed better than most of the other earth2observe models and this may  
438 be attributed to the fact that Lisflood has been extensively used in research and operational settings  
439 in Africa (Thiemig et al., 2015; Smith et al., 2020). As such, the model parameters may have been  
440 better constrained in the region than other models from earthH2Observe. Taking together, results from  
441 this study highlight the importance of evaluating outputs from WRR products in representative basins  
442 before applying them in studies that may have wider policy and financial implications in poorly  
443 gauged basins. Our results suggest a need to enhance the spatial resolution of WRR products and for  
444 the products to be driven by input data from multiple sources to reduce the uncertainties in the input  
445 data.

#### 446 **4.2. Evapotranspiration products**

447 The annual ET–precipitation ratio produced by WRR and satellite-based ET products are within the  
448 range estimated for the global land regions (Rodell et al., 2015) with the only exception being  
449 WaterGap, SSEBop, MOD16A2 and CR-ET with values beyond this range. This suggests that ET  
450 estimates from both sources performed well in this aspect. The annual ET–precipitation ratios  
451 obtained in this study show that annual ET does not exceed annual precipitation in most basins during  
452 the period under evaluation suggesting the availability of sufficient water resources in each basin.

453 Considering all the ET evaluation criteria and comparing between estimates from WRR and  
454 satellite-based products, FLDAS-Noah, Terra, GLEAM3.5a & 3.5b, and PMLV2 appear to  
455 outperform the rest of products even though GLEAM products slightly underestimated ET in all the  
456 basins. Conversely, WaterGap, SSEBop and MOD16A2 performed poorly and may not be suitable  
457 for water security assessment in the region. Our results are generally consistent with those from other  
458 studies indicating that GLEAM and MODIS16A2 underestimate evapotranspiration, while SSEBop  
459 overestimates this variable in most parts of Africa (Weerasinghe et al., 2020; Adeyeri and Ishola,  
460 2021; Mcnamara et al., 2021). Given that ET estimates from FLDAS-Noah is produced together with  
461 other water balance components (runoff, soil moisture and baseflow), outputs from this model may  
462 be recommended for water security assessment in the region because of water balance closure. Our  
463 results also revealed that the performance of satellite-based ET products is not influence by spatial  
464 resolution which is consistent with results from previous studies (Weerasinghe et al., 2020; Jiang and  
465 Liu, 2021). For example, Gleam products with a spatial resolution of 0.25° outperformed products  
466 such as MODIS16A2 and SSEBop with higher spatial resolutions. Conversely, ET estimates from

467 WRR appear to be influenced by spatial resolution considering that FLDAS-Noah and Terra with  
468 higher spatial resolutions outperformed other products with coarser resolutions.

469 Although all the products were able to capture the temporal dynamics of ET across all the  
470 basins, there were substantial discrepancies in the magnitude of monthly ET from each model. This  
471 finding is consistent with results from other studies showing strong differences in ET estimates  
472 produced by different models (Weerasinghe et al., 2020; Adeyeri and Ishola, 2021). The discrepancies  
473 in monthly ET estimates from the models may be attributed to differences in model structure,  
474 parameters, and uncertainties in the input data used in driving the models. This is also in-line with  
475 findings from another study in West Africa highlighting the impact of model parameters and input  
476 data uncertainty on ET estimates (Jung et al., 2019). Considering the aforementioned factors, it may  
477 be difficult to expect the products to produce similar results.

## 478 **5. Conclusions**

479 The objectives of this study were to assess the performance of water resources reanalysis and  
480 evapotranspiration products across eight basins in Africa. It should be noted the evaluation of the  
481 performance of WRR and ET products in this study did not explicitly consider the influence the  
482 models structure, parameters and input data on their performance. However, we do acknowledge that  
483 these factors could have significant impact on the performance of the different models evaluated.

484 The evaluation of WRR products for discharge simulation show varying strengths and  
485 weaknesses for the different models. Some models were able to capture the discharge dynamics in  
486 the basins while others could not adequately capture this pattern. Differences in the model  
487 performance can be attributed to differences model structure, parameters, input data used in driving  
488 the models and the spatial resolution of the WRR products. Apart from FLDAS-Noah which is a land  
489 surface model (LSM), our evaluation results show that global hydrological models (GHMs)  
490 performed better than LSMs except PCRGLOBW.

491 Evaluation of gridded ET products also revealed varying strengths and weaknesses for the  
492 different products. Based on the different evaluation criteria (bias, RMSE, Pearson correlation  
493 coefficient, and temporal ET variability), FLDAS-Noah appears to outperform most of other ET  
494 estimates and may therefore be recommended for water security assessment in the region. More so,  
495 because of water balance closure and the availability of other water balance components (runoff, soil  
496 moisture and baseflow). Our results also suggest that the performance of satellite-based ET products  
497 is not influenced by spatial resolution, while differences in ET estimates may be attributed to  
498 differences in model structure, parameters and the input data used to drive each ET model. On the  
499 contrary, spatial resolution appears to have a significant impact on the performance of WRR in  
500 simulating ET estimates.

501 Results from this study suggest that WRR and ET products may be used for water security  
502 assessment in poorly gauged basins. However, it is imperative to evaluate the performance of these  
503 products in representative gauged basins before applying them in poorly gauged basins. This is  
504 because applying the products in poorly gauged basins without evaluating their performance may  
505 lead to poor water management decisions with wider policy and financial implications. There is also  
506 a need for WRR and ET products to be driven by input data from multiple sources to reduce  
507 uncertainties in the input data. Furthermore, the spatial resolution of WRR products needs to be  
508 enhanced given that models with higher spatial resolutions outperformed those with coarser  
509 resolutions. Results from this study may be used by the products developers to improve on the quality  
510 of future WRR and ET products.

511 **Author contributions:** EN and RGB designed the methodological framework and contributed to the  
512 entire strategic and conceptual framework of the study. EN prepared the data, performed the analyses,  
513 interpreted the results and wrote the original draft. JN and EIB provided discharge data for the Mono  
514 and Oueme basins respectively. All authors read the paper and provided feedback.

515 **Competing interests:** The authors declare that they have no conflict of interest.

516 **Acknowledgements:** E.N. was funded by the Leverhulme Trust Early Career Fellowship – Award  
517 Number ECF–097–2020. We are grateful to Coralie Adams at Manchester University for writing the  
518 Python code that was used to produce Figures 4 & 8.

## 519 **References**

- 520 Abatzoglou, J. T., Dobrowski, S. Z., Parks, S. A., and Hegewisch, K. C.: TerraClimate, a high-  
521 resolution global dataset of monthly climate and climatic water balance from 1958–2015,  
522 *Scientific data*, 5, 1-12, <https://doi.org/10.1038/sdata.2017.191>, 2018.
- 523 Adeyeri, O. E. and Ishola, K. A.: Variability and Trends of Actual Evapotranspiration over West  
524 Africa: The Role of Environmental Drivers, *Agricultural and Forest Meteorology*, 308-309,  
525 108574, <https://doi.org/10.1016/j.agrformet.2021.108574>, 2021.
- 526 Andam-Akorful, S. A., Ferreira, V. G., Awange, J. L., Forootan, E., and He, X. F.: Multi-model and  
527 multi-sensor estimations of evapotranspiration over the Volta Basin, West Africa,  
528 *International Journal of Climatology*, 35, 3132-3145, <https://doi.org/10.1002/joc.4198>, 2015.
- 529 Ashouri, H., Hsu, K.-L., Sorooshian, S., Braithwaite, D. K., Knapp, K. R., Cecil, L. D., Nelson, B.  
530 R., and Prat, O. P.: PERSIANN-CDR: Daily precipitation climate data record from  
531 multisatellite observations for hydrological and climate studies, *Bulletin of the American*  
532 *Meteorological Society*, 96, 69-83, 2015.
- 533 Balsamo, G., Beljaars, A., Scipal, K., Viterbo, P., van den Hurk, B., Hirschi, M., and Betts, A. K.: A  
534 revised hydrology for the ECMWF model: Verification from field site to terrestrial water  
535 storage and impact in the Integrated Forecast System, *Journal of hydrometeorology*, 10, 623-  
536 643, <https://doi.org/10.1175/2008JHM1068.1>, 2009.
- 537 Biancamaria, S., Mballo, M., Le Moigne, P., Sánchez Pérez, J. M., Espitalier-Noël, G., Grusson, Y.,  
538 Cakir, R., Häfliger, V., Barathieu, F., Trasmonte, M., Boone, A., Martin, E., and Sauvage, S.:  
539 Total water storage variability from GRACE mission and hydrological models for a 50,000

540 km<sup>2</sup> temperate watershed: the Garonne River basin (France), *Journal of Hydrology: Regional*  
541 *Studies*, 24, 100609, <https://doi.org/10.1016/j.ejrh.2019.100609>, 2019.

542 Blatchford, M. L., Mannaerts, C. M., Njuki, S. M., Nouri, H., Zeng, Y., Pelgrum, H., Wonink, S., and  
543 Karimi, P.: Evaluation of WaPOR V2 evapotranspiration products across Africa,  
544 *Hydrological processes*, 34, 3200-3221, <https://doi.org/10.1002/hyp.13791>, 2020.

545 Byers, E., Gidden, M., Leclère, D., Balkovic, J., Burek, P., Ebi, K., Greve, P., Grey, D., Havlik, P.,  
546 and Hillers, A.: Global exposure and vulnerability to multi-sector development and climate  
547 change hotspots, *Environmental Research Letters*, 13, 055012, [https://doi.org/10.1088/1748-](https://doi.org/10.1088/1748-9326/aabf45)  
548 [9326/aabf45](https://doi.org/10.1088/1748-9326/aabf45), 2018.

549 Couasnon, A., Eilander, D., Muis, S., Veldkamp, T. I., Haigh, I. D., Wahl, T., Winsemius, H. C., and  
550 Ward, P. J.: Measuring compound flood potential from river discharge and storm surge  
551 extremes at the global scale, *Natural Hazards and Earth System Sciences*, 20, 489-504,  
552 <https://doi.org/10.5194/nhess-20-489-2020>, 2020.

553 Decharme, B., Alkama, R., Douville, H., Becker, M., and Cazenave, A.: Global Evaluation of the  
554 ISBA-TRIP Continental Hydrological System. Part II: Uncertainties in River Routing  
555 Simulation Related to Flow Velocity and Groundwater Storage, *Journal of*  
556 *Hydrometeorology*, 11, 601-617, <https://doi.org/10.1175/2010JHM1212.1>, 2010.

557 Dembélé, M., Schaeffli, B., Van De Giesen, N., and Mariéthoz, G.: Suitability of 17 gridded rainfall  
558 and temperature datasets for large-scale hydrological modelling in West Africa, *Hydrology*  
559 *and earth system sciences*, 24, 5379-5406, 2020.

560 Dinku, T., Funk, C., Peterson, P., Maidment, R., Tadesse, T., Gadain, H., and Ceccato, P.: Validation  
561 of the CHIRPS satellite rainfall estimates over eastern Africa, *Quarterly Journal of the Royal*  
562 *Meteorological Society*, 144, 292-312, <https://doi.org/10.1002/qj.3244>, 2018.

563 Flörke, M., Schneider, C., and McDonald, R. I.: Water competition between cities and agriculture  
564 driven by climate change and urban growth, *Nature Sustainability*, 1, 51-58,  
565 <https://doi.org/10.1038/s41893-017-0006-8>, 2018.

566 Funk, C., Peterson, P., Landsfeld, M., Pedreros, D., Verdin, J., Shukla, S., Husak, G., Rowland, J.,  
567 Harrison, L., and Hoell, A.: The climate hazards infrared precipitation with stations—a new  
568 environmental record for monitoring extremes, *Scientific data*, 2, 1-21,  
569 <https://doi.org/10.1038/sdata.2015.66>, 2015.

570 Gründemann, G. J., Werner, M., and Veldkamp, T. I.: The potential of global reanalysis datasets in  
571 identifying flood events in Southern Africa, *Hydrology and Earth System Sciences*, 22, 4667-  
572 4683, <https://doi.org/10.1038/sdata.2015.66>, 2018.

573 Gupta, H. V., Kling, H., Yilmaz, K. K., and Martinez, G. F.: Decomposition of the mean squared  
574 error and NSE performance criteria: Implications for improving hydrological modelling,  
575 *Journal of Hydrology*, 377, 80-91, <https://doi.org/10.1016/j.jhydrol.2009.08.003>, 2009.

576 Harrigan, S., Zsoter, E., Alfieri, L., Prudhomme, C., Salamon, P., Wetterhall, F., Barnard, C., Cloke,  
577 H., and Pappenberger, F.: GloFAS-ERA5 operational global river discharge reanalysis 1979–  
578 present, *Earth System Science Data*, 12, 2043-2060, [https://doi.org/10.5194/essd-12-2043-](https://doi.org/10.5194/essd-12-2043-2020)  
579 [2020](https://doi.org/10.5194/essd-12-2043-2020), 2020.

580 Hirpa, F. A., Alfieri, L., Lees, T., Peng, J., Dyer, E., and Dadson, S. J.: Streamflow response to climate  
581 change in the Greater Horn of Africa, *Climatic Change*, 156, 341-363,  
582 <https://doi.org/10.1007/s10584-019-02547-x>, 2019.

583 Jiang, Y. and Liu, Z.: Evaluations of Remote Sensing-Based Global Evapotranspiration Datasets at  
584 Catchment Scale in Mountain Regions, *Remote Sensing*, 13, 5096,  
585 <https://doi.org/10.3390/rs13245096>, 2021.

586 Jung, H. C., Getirana, A., Arsenault, K. R., Holmes, T. R. H., and McNally, A.: Uncertainties in  
587 Evapotranspiration Estimates over West Africa, *Remote Sensing*, 11, 892,  
588 <https://doi.org/10.3390/rs11080892>, 2019.

589 Kabuya, P. M., Hughes, D. A., Tshimanga, R. M., Trigg, M. A., and Bates, P.: Establishing  
590 uncertainty ranges of hydrologic indices across climate and physiographic regions of the

591 Congo River Basin, *Journal of Hydrology: Regional Studies*, 30, 100710,  
592 <https://doi.org/10.1016/j.ejrh.2020.100710>, 2020.

593 Koukoula, M., Nikolopoulos, E. I., Dokou, Z., and Anagnostou, E. N.: Evaluation of global water  
594 resources reanalysis products in the upper Blue Nile River Basin, *Journal of*  
595 *Hydrometeorology*, 21, 935-952, <https://doi.org/10.1175/JHM-D-19-0233.1>, 2020.

596 Krabbenhoft, C. A., Allen, G. H., Lin, P., Godsey, S. E., Allen, D. C., Burrows, R. M., DelVecchia,  
597 A. G., Fritz, K. M., Shanafield, M., Burgin, A. J., Zimmer, M. A., Datry, T., Dodds, W. K.,  
598 Jones, C. N., Mims, M. C., Franklin, C., Hammond, J. C., Zipper, S., Ward, A. S., Costigan,  
599 K. H., Beck, H. E., and Olden, J. D.: Assessing placement bias of the global river gauge  
600 network, *Nature Sustainability*, 2022.

601 Krinner, G., Viovy, N., de Noblet-Ducoudré, N., Ogée, J., Polcher, J., Friedlingstein, P., Ciais, P.,  
602 Sitch, S., and Prentice, I. C.: A dynamic global vegetation model for studies of the coupled  
603 atmosphere-biosphere system, *Global Biogeochemical Cycles*, 19,  
604 <https://doi.org/10.1029/2003GB002199>, 2005.

605 Laipelt, L., Kayser, R. H. B., Fleischmann, A. S., Ruhoff, A., Bastiaanssen, W., Erickson, T. A., and  
606 Melton, F.: Long-term monitoring of evapotranspiration using the SEBAL algorithm and  
607 Google Earth Engine cloud computing, *ISPRS Journal of Photogrammetry and Remote*  
608 *Sensing*, 178, 81-96, <https://doi.org/10.1016/j.isprsjprs.2021.05.018>, 2021.

609 Lakew, H. B., Moges, S. A., Anagnostou, E. N., Nikolopoulos, E. I., and Asfaw, D. H.: Evaluation  
610 of global water resources reanalysis runoff products for local water resources applications:  
611 case study-upper Blue Nile basin of Ethiopia, *Water Resources Management*, 34, 2157-2177,  
612 <https://doi.org/10.1007/s11269-019-2190-y>, 2020.

613 Larbi, I., Hountondji, F. C. C., Dotse, S.-Q., Mama, D., Nyamekye, C., Adeyeri, O. E., Djan'na  
614 Koubodana, H., Odoom, P. R. E., and Asare, Y. M.: Local climate change projections and  
615 impact on the surface hydrology in the Vea catchment, West Africa, *Hydrology Research*, 52,  
616 1200-1215, <https://doi.org/10.2166/nh.2021.096>, 2021.

617 Liu, W.: Evaluating remotely sensed monthly evapotranspiration against water balance estimates at  
618 basin scale in the Tibetan Plateau, *Hydrology Research*, 49, 1977-1990, 10.2166/nh.2018.008,  
619 2018.

620 López, P. L., Sultana, T., Kafi, M. A. H., Hossain, M. S., Khan, A. S., and Masud, M. S.: Evaluation  
621 of global water resources reanalysis data for estimating flood events in the Brahmaputra River  
622 Basin, *Water Resources Management*, 34, 2201-2220, <https://doi.org/10.1007/s11269-020-02546-z>, 2020.

624 Ma, N., Szilagyi, J., and Zhang, Y.: Calibration-free complementary relationship estimates terrestrial  
625 evapotranspiration globally, *Water Resources Research*, 57, e2021WR029691, 2021.

626 Martens, B., Miralles, D. G., Lievens, H., Van Der Schalie, R., De Jeu, R. A., Fernández-Prieto, D.,  
627 Beck, H. E., Dorigo, W. A., and Verhoest, N. E.: GLEAM v3: Satellite-based land evaporation  
628 and root-zone soil moisture, *Geoscientific Model Development*, 10, 1903-1925,  
629 <https://doi.org/10.5194/gmd-10-1903-2017>, 2017.

630 McNally, A., Arsenault, K., Kumar, S., Shukla, S., Peterson, P., Wang, S., Funk, C., Peters-Lidard,  
631 C. D., and Verdin, J. P.: A land data assimilation system for sub-Saharan Africa food and  
632 water security applications, *Scientific data*, 4, 1-19, <https://doi.org/10.1038/sdata.2017.12>,  
633 2017.

634 McNamara, I., Baez-Villanueva, O. M., Zomorodian, A., Ayyad, S., Zambrano-Bigiarini, M., Zaroug,  
635 M., Mersha, A., Nauditt, A., Mbuliro, M., and Wamala, S.: How well do gridded precipitation  
636 and actual evapotranspiration products represent the key water balance components in the  
637 Nile Basin?, *Journal of Hydrology: Regional Studies*, 37, 100884,  
638 <https://doi.org/10.1016/j.ejrh.2021.100884>, 2021.

639 Moriasi, D., G. Arnold, J., W. Van Liew, M., L. Bingner, R., D. Harmel, R., and L. Veith, T.: Model  
640 Evaluation Guidelines for Systematic Quantification of Accuracy in Watershed Simulations,  
641 *Transactions of the ASABE*, 50, 885-900, <https://doi.org/10.13031/2013.23153>, 2007.

642 Mu, Q., Zhao, M., and Running, S. W.: Improvements to a MODIS global terrestrial  
643 evapotranspiration algorithm, *Remote sensing of environment*, 115, 1781-1800,  
644 <https://doi.org/10.1016/j.rse.2011.02.019>, 2011.

645 Mu, Q., Heinsch, F. A., Zhao, M., and Running, S. W.: Development of a global evapotranspiration  
646 algorithm based on MODIS and global meteorology data, *Remote sensing of Environment*,  
647 111, 519-536, <https://doi.org/10.1016/j.rse.2007.04.015>, 2007.

648 Neal, J., Schumann, G., Bates, P., Buytaert, W., Matgen, P., and Pappenberger, F.: A data assimilation  
649 approach to discharge estimation from space, *Hydrological Processes*, 23, 3641-3649,  
650 <https://doi.org/10.1002/hyp.7518>, 2009.

651 Nkiaka, E.: Water security assessment in ungauged regions using the water balance and water  
652 footprint concepts and satellite observations, *Hydrology Research*,  
653 <https://doi.org/10.2166/nh.2022.124>, 2022.

654 Nkiaka, E., Nawaz, N., and Lovett, J.: Using self-organizing maps to infill missing data in hydro-  
655 meteorological time series from the Logone catchment, Lake Chad basin, *Environmental*  
656 *Monitoring and Assessment*, 188, 1-12, <https://doi.org/10.1007/s10661-016-5385-1>, 2016.

657 Nkiaka, E., Bryant, R. G., Okumah, M., and Gomo, F. F.: Water security in sub-Saharan Africa:  
658 Understanding the status of sustainable development goal 6, *WIREs Water*, 8, e1552,  
659 <https://doi.org/10.1002/wat2.1552>, 2021.

660 Nkiaka, E., Taylor, A., Dougill, A. J., Antwi-Agyei, P., Adefisan, E. A., Ahiataku, M. A., Baffour-  
661 Ata, F., Fournier, N., Indasi, V. S., and Konte, O.: Exploring the need for developing impact-  
662 based forecasting in West Africa, *Frontiers in Climate*, 11,  
663 <https://doi.org/10.3389/fclim.2020.565500>, 2020.

664 Odusanya, A. E., Mehdi, B., Schürz, C., Oke, A. O., Awokola, O. S., Awomeso, J. A., Adejuwon, J.  
665 O., and Schulz, K.: Multi-site calibration and validation of SWAT with satellite-based  
666 evapotranspiration in a data-sparse catchment in southwestern Nigeria, *Hydrology and Earth*  
667 *System Sciences*, 23, 1113-1144, <https://doi.org/10.5194/hess-23-1113-2019>, 2019.

668 Oussou, F. E., Ndehedehe, C. E., Oloukoi, J., Yalo, N., Boukari, M., and Diaw, A. T.:  
669 Characterization of the hydro-geological regime of fractured aquifers in Benin (West-Africa)  
670 using multi-satellites and models, *Journal of Hydrology: Regional Studies*, 39, 100987,  
671 <https://doi.org/10.1016/j.ejrh.2021.100987>, 2022.

672 Rodell, M., Houser, P., Jambor, U., Gottschalck, J., Mitchell, K., Meng, C.-J., Arsenault, K.,  
673 Cosgrove, B., Radakovich, J., and Bosilovich, M.: The global land data assimilation system,  
674 *Bulletin of the American Meteorological society*, 85, 381-394,  
675 <https://doi.org/10.1175/BAMS-85-3-381>, 2004.

676 Rodell, M., Beaudoin, H. K., L'Ecuyer, T. S., Olson, W. S., Famiglietti, J. S., Houser, P. R., Adler,  
677 R., Bosilovich, M. G., Clayson, C. A., Chambers, D., Clark, E., Fetzer, E. J., Gao, X., Gu, G.,  
678 Hilburn, K., Huffman, G. J., Lettenmaier, D. P., Liu, W. T., Robertson, F. R., Schlosser, C.  
679 A., Sheffield, J., and Wood, E. F.: The Observed State of the Water Cycle in the Early Twenty-  
680 First Century, *Journal of Climate*, 28, 8289-8318, <https://doi.org/10.1175/JCLI-D-14-00555.1>, 2015.

682 Rodríguez, E., Sánchez, I., Duque, N., Arboleda, P., Vega, C., Zamora, D., López, P., Kaune, A.,  
683 Werner, M., and García, C.: Combined use of local and global hydro meteorological data with  
684 hydrological models for water resources management in the Magdalena-Cauca Macro Basin-  
685 Colombia, *Water Resources Management*, 34, 2179-2199, <https://doi.org/10.1007/s11269-019-02236-5>, 2020.

687 Saha, S., Moorthi, S., Wu, X., Wang, J., Nadiga, S., Tripp, P., Behringer, D., Hou, Y.-T., Chuang,  
688 H.-y., and Iredell, M.: The NCEP climate forecast system version 2, *Journal of climate*, 27,  
689 2185-2208, <https://doi.org/10.1175/JCLI-D-12-00823.1>, 2014.

690 Satgé, F., Defrance, D., Sultan, B., Bonnet, M.-P., Seyler, F., Rouché, N., Pierron, F., and Paturel, J.-  
691 E.: Evaluation of 23 gridded precipitation datasets across West Africa, *Journal of Hydrology*,  
692 581, 124412, <https://doi.org/10.1016/j.jhydrol.2019.124412>, 2020.

693 Schellekens, J., Dutra, E., Martínez-de la Torre, A., Balsamo, G., Van Dijk, A., Sperna Weiland, F.,  
694 Minvielle, M., Calvet, J.-C., Decharme, B., and Eisner, S.: A global water resources ensemble  
695 of hydrological models: the earthH2Observe Tier-1 dataset, *Earth System Science Data*, 9, 389-  
696 413, <https://doi.org/10.5194/essd-9-389-2017>, 2017.

697 Senay, G. B., Bohms, S., Singh, R. K., Gowda, P. H., Velpuri, N. M., Alemu, H., and Verdin, J. P.:  
698 Operational evapotranspiration mapping using remote sensing and weather datasets: A new  
699 parameterization for the SSEB approach, *JAWRA Journal of the American Water Resources  
700 Association*, 49, 577-591, <https://doi.org/10.1111/jawr.12057>, 2013.

701 Sheffield, J., Wood, E. F., Pan, M., Beck, H., Coccia, G., Serrat-Capdevila, A., and Verbist, K.:  
702 Satellite remote sensing for water resources management: Potential for supporting sustainable  
703 development in data-poor regions, *Water Resources Research*, 54, 9724-9758,  
704 <https://doi.org/10.1029/2017WR022437>, 2018.

705 Sikder, M., David, C. H., Allen, G. H., Qiao, X., Nelson, E. J., and Matin, M. A.: Evaluation of  
706 available global runoff datasets through a river model in support of transboundary water  
707 management in South and Southeast Asia, *Frontiers in Environmental Science*, 171,  
708 <https://doi.org/10.3389/fenvs.2019.00171>, 2019.

709 Skofronick-Jackson, G., Berg, W., Kidd, C., Kirschbaum, D. B., Petersen, W. A., Huffman, G. J., and Takayabu,  
710 Y. N.: Global precipitation measurement (GPM): Unified precipitation estimation from space, in:  
711 *Remote Sensing of Clouds and Precipitation*, Springer, 175-193, 2018.

712 Slater, L. J., Anderson, B., Buechel, M., Dadson, S., Han, S., Harrigan, S., Kelder, T., Kowal, K.,  
713 Lees, T., and Matthews, T.: Nonstationary weather and water extremes: a review of methods  
714 for their detection, attribution, and management, *Hydrology and Earth System Sciences*, 25,  
715 3897-3935, <https://doi.org/10.5194/hess-25-3897-2021>, 2021.

716 Smith, M. W., Willis, T., Alfieri, L., James, W. H. M., Trigg, M. A., Yamazaki, D., Hardy, A. J.,  
717 Bisselink, B., De Roo, A., Macklin, M. G., and Thomas, C. J.: Incorporating hydrology into  
718 climate suitability models changes projections of malaria transmission in Africa, *Nature  
719 Communications*, 11, 4353, <https://doi.org/10.1038/s41467-020-18239-5>, 2020.

720 Tapley, B. D., Watkins, M. M., Flechtner, F., Reigber, C., Bettadpur, S., Rodell, M., Sasgen, I.,  
721 Famiglietti, J. S., Landerer, F. W., Chambers, D. P., Reager, J. T., Gardner, A. S., Save, H.,  
722 Ivins, E. R., Swenson, S. C., Boening, C., Dahle, C., Wiese, D. N., Dobslaw, H., Tamisiea,  
723 M. E., and Velicogna, I.: Contributions of GRACE to understanding climate change, *Nature  
724 Climate Change*, 9, 358-369, <https://doi.org/10.1038/s41558-019-0456-2>, 2019.

725 Thiemi, V., Bisselink, B., Pappenberger, F., and Thielen, J.: A pan-African medium-range ensemble  
726 flood forecast system, *Hydrol. Earth Syst. Sci.*, 19, 3365-3385, [https://doi.org/10.5194/hess-  
727 19-3365-2015](https://doi.org/10.5194/hess-19-3365-2015), 2015.

728 UNDESA: United Nations, Department of Economic and Social Affairs, Population Division Prospects, Volume  
729 I: Comprehensive Tables (ST/ESA/SER.A/426), 2019.

730 van Beek, L. P. H., Wada, Y., and Bierkens, M. F. P.: Global monthly water stress: 1. Water balance  
731 and water availability, *Water Resources Research*, 47,  
732 <https://doi.org/10.1029/2010WR009791>, 2011.

733 Van Der Knijff, J. M., Younis, J., and De Roo, A. P. J.: LISFLOOD: a GIS-based distributed model  
734 for river basin scale water balance and flood simulation, *International Journal of Geographical  
735 Information Science*, 24, 189-212, 10.1080/13658810802549154, 2010.

736 van Dijk, A. I. J. M., Renzullo, L. J., Wada, Y., and Tregoning, P.: A global water cycle reanalysis  
737 (2003&ndash;2012) merging satellite gravimetry and altimetry observations with a  
738 hydrological multi-model ensemble, *Hydrol. Earth Syst. Sci.*, 18, 2955-2973,  
739 <https://doi.org/10.5194/hess-18-2955-2014>, 2014.

740 Wada, Y., Wisser, D., and Bierkens, M. F. P.: Global modeling of withdrawal, allocation and  
741 consumptive use of surface water and groundwater resources, *Earth Syst. Dynam.*, 5, 15-40,  
742 <https://doi.org/10.5194/esd-5-15-2014>, 2014.

743 Weedon, G. P., Balsamo, G., Bellouin, N., Gomes, S., Best, M. J., and Viterbo, P.: The WFDEI  
744 meteorological forcing data set: WATCH Forcing Data methodology applied to ERA-Interim

745 reanalysis data, *Water Resources Research*, 50, 7505-7514,  
746 <https://doi.org/10.1002/2014WR015638>, 2014.

747 Weerasinghe, I., Bastiaanssen, W., Mul, M., Jia, L., and Van Griensven, A.: Can we trust remote  
748 sensing evapotranspiration products over Africa?, *Hydrology and Earth System Sciences*, 24,  
749 1565-1586, <https://doi.org/10.5194/hess-24-1565-2020>, 2020.

750 Wiese, D. N., Landerer, F. W., and Watkins, M. M.: Quantifying and reducing leakage errors in the  
751 JPL RL05M GRACE mascon solution, *Water Resources Research*, 52, 7490-7502,  
752 <https://doi.org/10.1002/2016WR019344>, 2016.

753 Xie, J., Liu, L., Wang, Y., Xu, Y.-P., and Chen, H.: Changes in actual evapotranspiration and its  
754 dominant drivers across the Three-River Source Region of China during 1982–2014,  
755 *Hydrology Research*, <https://doi.org/10.2166/nh.2022.076>, 2022.

756 Zhang, Y., Kong, D., Gan, R., Chiew, F. H. S., McVicar, T. R., Zhang, Q., and Yang, Y.: Coupled  
757 estimation of 500 m and 8-day resolution global evapotranspiration and gross primary  
758 production in 2002–2017, *Remote Sensing of Environment*, 222, 165-182,  
759 <https://doi.org/10.1016/j.rse.2018.12.031>, 2019.

760 Zhang, Y., Peña-Arancibia, J. L., McVicar, T. R., Chiew, F. H., Vaze, J., Liu, C., Lu, X., Zheng, H.,  
761 Wang, Y., and Liu, Y. Y.: Multi-decadal trends in global terrestrial evapotranspiration and its  
762 components, *Scientific reports*, 6, 1-12, <https://doi.org/10.1038/srep19124>, 2016.

763